Transactions on Ecology and the Environment vol 12, © 1996 WIT Press, www.witpress.com, ISSN 1743-3541

A boundary integral technique for free surface flows under gravity

X. Wen, K. Manik, D.B. Ingham
Department of Applied Mathematical Studies, University of Leeds, Leeds LS2 9JT, UK

Abstract

A boundary integral technique has been developed for two-dimensional, free surface flows in complex geometries in hydraulic engineering. Based on the assumption of steady, ideal, irrotational flow in a channel a system of integral equations, which are valid on the boundaries of the solution domain, have been derived using the theory for mixed-boundary problems of an analytical function. The boundary integral equations are solved for the velocities on the solid boundary and the free surface, the shape of the free surface and for the the critical Froude number for which waves first occur.

1 Introduction

The free surface flow of an incompressible, irrotational and inviscid fluid under the force of gravity has been the subject of considerable research in hydraulic engineering over many years. In last three decades both the finite element method and the boundary element method[1,2] have used to solve the free surface flows over complex geometries in numerous hydraulic engineering applications. King and Bloor[3] considered the steady, two-dimensional free-surface flow of an incompressible, irrotational and inviscid fluid flow over a fixed solid rectangular step using the conformal mapping technique, based on a modified Schwartz-Christoffel transformation. Through the use of the exact free-surface condition a non-linear, integro-differential equation was formulated and solved for the free surface flow over a step when the upstream flow is both supercritical and subcritical. Forbes[4], who used a boundary-integral method, investigated the flow over a semi-circular obstruction in a channel, whilst Dias and Vanden-Broeck[5] obtained solutions

to both subcritical and supercritical free-surface flows past a triangular obstacle by a series truncation method. In this paper a numerical boundary integral technique, as developed by Wen and Wu[6] and Wen and Ingham[7], has been employed to study the free-surface flow over a step in a channel.

2 Formulation of the boundary-integral equation

In this paper we consider the gravity-influenced two-dimensional steady, inviscid and irrotational fluid flow over a step in channel. At large distance upstream of the step the flow has a constant speed of U_∞ and the depth of the fluid is h and the fluid flows horizontally in the positive x direction. At $x = 0$ there is a step which is inclined to the horizontal at an angle β until it reaches a height h_s and then the surface is horizontal. Figure 1a schematically shows the physical situation investigated, where $A'_\infty D'_\infty$ is the upper free-surface of the flow, the solid boundaries $A_\infty B$ and CD_∞ are horizontal and BC is a straight line at an angle β to the x axis. Without any loss of generality we choose the streamfunction ψ=0 on the solid boundary and then $\psi = q = hU_\infty$ on the free surface $A'_\infty D'_\infty$.

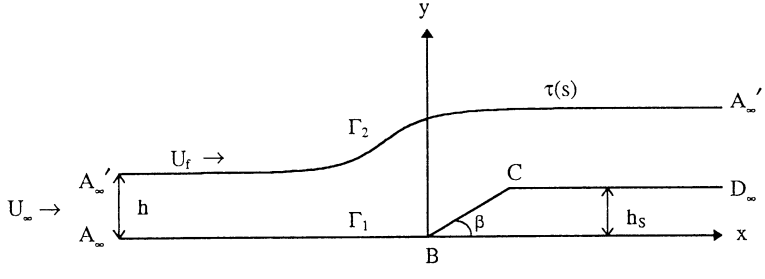

Figure 1a: The free surface flow over a step.

A coordinate system $z = x + iy$ is introduced with the x axis along $A_\infty B$ and y is measured vertically upwards. The complex velocity potential is defined by $w = \phi + i\psi$, where ϕ is the velocity potential. Along the free surface $A'_\infty D'_\infty$ we apply Bernoulli's equation which gives

$$y_f + u_f^2/(2g) = h + U_\infty^2/(2g) \tag{1}$$

or

$$u_f/U_\infty = \sqrt{1 + 2(1 - y_f/h)/F_\tau^2} \tag{2}$$

where u_f is the fluid speed on the free surface, $F_\tau = U_\infty/\sqrt{gh}$ is the upstream Froude number, and g is the acceleration due to gravity.

We next consider the complex velocity

$$dw/dz = ue^{-i\theta} \tag{3}$$

in which u is the fluid speed and θ is the angle that the fluid velocity vector makes with the positive x axis. Then we obtain

$$\Omega = ln(\frac{1}{U_\infty}\frac{dw}{dz}) = ln[\frac{u}{U_\infty}e^{-i\theta}] = \tau - i\theta \tag{4}$$

where Ω is the logarithm of the complex velocity and $\tau = ln(u/U_\infty)$, and τ, dw/dz and Ω are analytical functions in a strip of the w-plane, see Figure 1b.

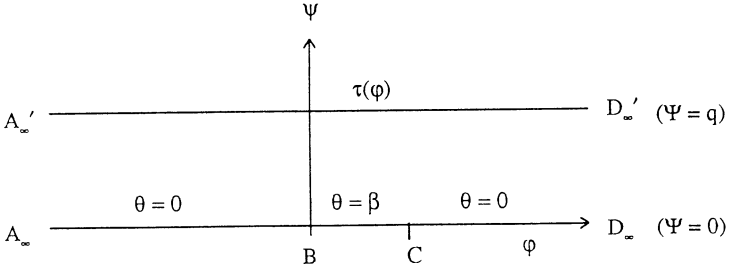

Figure 1b: The w-plane.

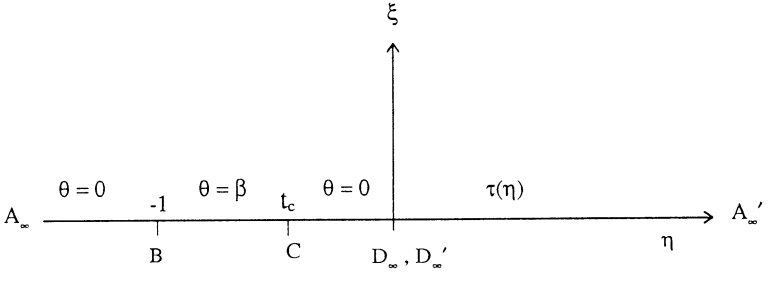

Figure 1c: The t-plane.

The infinite strip in the complex w-plane is now transformed onto the upper half-plane of the auxiliary plane, namely $t = \zeta + i\eta$, by applying the mapping function, see Figure 1c, namely

$$t = -e^{-\frac{\pi}{q}w} \tag{5}$$

For the Riemann-Hilbert mixed boundary-value problem[8], the boundary conditions on the real ζ axis of the t-plane are as follows:

$$On \quad A_\infty B \quad (\zeta < -1), \qquad \Im m\Omega(\zeta) = 0, \tag{6}$$

$$On \quad BC \quad (-1 < \zeta < t_c), \qquad \Im m\Omega(\zeta) = -\beta \tag{7}$$

$$On \quad CD \quad (t_c < \zeta < 0), \qquad \Im m\Omega(\zeta) = 0 \tag{8}$$

$$On \quad D'_\infty A'_\infty \qquad (0 < \zeta < \infty), \qquad \Re e\Omega(\zeta) = \tau(\zeta) \tag{9}$$

By referring to the general solution of the Riemann-Hilbert problem[8] we obtain the solution of Ω in the form

$$\Omega(t) = \frac{X(t)}{\pi}\left[\int_{-1}^{t_c} \frac{-\beta}{\sqrt{-\zeta}(\zeta - t)} d\zeta + \int_0^{t_\infty} \frac{\tau(\zeta)}{\sqrt{\zeta}(\zeta - t)} d\zeta\right] \tag{10}$$

where $X(t) = (\sqrt{-t})$ is the homogeneous solution of $\Omega(t)$ when its real part, $\Re e\Omega$, and the imaginary part, $\Im m\Omega$, are equal to zero on the real axis ζ. When t approaches the real axis ζ from the upper half plane, the value of $X(t)$ on the real axis ζ is given by

$$X^+(\zeta) = \sqrt{-\zeta} \qquad \zeta < 0 \tag{11}$$

$$X^+(\zeta) = -i\sqrt{\zeta} \qquad \zeta > 0 \tag{12}$$

On taking the Cauchy Principle Value and separating the real and imaginary parts of $\Omega(\zeta_0)$, the velocity on the solid boundary $A_\infty D_\infty$ is:

$$\tau(\zeta_0) = \frac{\sqrt{-\zeta}}{\pi}\left[\int_{-1}^{t_c} \frac{-\beta}{\sqrt{-\zeta}(\zeta - \zeta_0)} d\zeta + \int_0^{t_\infty} \frac{\tau(\zeta)}{\sqrt{\zeta}(\zeta - \zeta_0)} d\zeta\right] \quad \zeta < 0 \tag{13}$$

and the angle that the free surface $A'_\infty D'_\infty$ makes with the horizontal is

$$\theta(\zeta_0) = \frac{\sqrt{\zeta}}{\pi}\left[\int_{-1}^{t_c} \frac{-\beta}{\sqrt{-\zeta}(\zeta - \zeta_0)} d\zeta + \int_0^{t_\infty} \frac{\tau(\zeta)}{\sqrt{\zeta}(\zeta - \zeta_0)} d\zeta\right] \qquad \zeta > 0 \tag{14}$$

Now we take the arc length s to be the independent variable. Thus we have, from equation (5),

$$d\zeta = \frac{\pi}{q} e^{-\frac{\pi}{q}\phi(s)} u(s) ds \quad on \ \Gamma_1 \tag{15}$$

$$d\zeta = -\frac{\pi}{q} e^{-\frac{\pi}{q}\phi(s)} u(s) ds \quad on \ \Gamma_2 \tag{16}$$

where Γ_1 and Γ_2 are the solid boundary $A_\infty D_\infty$ and the free surface $A'_\infty D'_\infty$, respectively. Along the free surface and solid boundary we have

$$d\phi(s)/ds = u(s) \tag{17}$$

which on integration gives

$$\phi(s) = \phi_A + \int_0^s u(l) dl \tag{18}$$

where we have taken the value of the potential function at the points A and A′ to be equal and ϕ_A to be the value at the point A_∞.

The coordinates of the free surface are then given by

$$x(s) = x_{A'} + \int_0^s cos\theta(l)dl \tag{19}$$

and

$$y(s) = y_{A'} + \int_0^s sin\theta(l)dl \tag{20}$$

where $y_{A'}$ and $x_{A'}$ are the coordinates of the point A'_∞.

In the physical plane we may rewrite equations (13) and (14) as follows:

$$\begin{aligned}\tau(s) &= ln\frac{u(s)}{U_\infty} = \frac{\sqrt{-\zeta(s)}}{q}\left[\int_{\Gamma_1}\frac{-\beta}{\sqrt{-\zeta(l)}[\zeta(l)-\zeta(s)]}e^{-\frac{\pi}{q}\phi(l)}u(l)dl\right] \\ &\quad -\left[\int_{\Gamma_2}\frac{\tau(l)}{\sqrt{\zeta(l)}[\zeta(l)-\zeta(s)]}e^{-\frac{\pi}{q}\phi(l)}u(l)dl\right] \qquad s\in\Gamma_1\end{aligned} \tag{21}$$

$$\begin{aligned}\theta(s) &= \frac{\sqrt{\zeta(s)}}{q}\left[\int_{\Gamma_1}\frac{-\beta}{\sqrt{-\zeta(l)}[\zeta(l)-\zeta(s)]}e^{-\frac{\pi}{q}\phi(l)}u(l)dl\right] \\ &\quad -\left[\int_{\Gamma_2}\frac{\tau(l)}{\sqrt{\zeta(l)}[\zeta(l)-\zeta(s)]}e^{-\frac{\pi}{q}\phi(l)}u(l)dl\right] \qquad s\in\Gamma_2\end{aligned} \tag{22}$$

in which

$$\zeta(l) = -e^{-\frac{\pi}{q}\phi(l)} \qquad on\ \ \Gamma_1 \tag{23}$$

$$\zeta(l) = e^{-\frac{\pi}{q}\phi(l)} \qquad on\ \ \Gamma_2 \tag{24}$$

In equations (21) and (22), $\tau(l)$ is calculated by using equation (2), namely,

$$\tau(l) = ln[u_f(l)/U_\infty] = ln\sqrt{1+2[1-y_f(l)/h]/F_\tau^2} \tag{25}$$

The equations (18)-(22) are the boundary integral equations for the potential function $\phi(s)$ on the boundaries, the coordinates of the free surface, $x(s)$ and $y(s)$, the fluid speed, $u(s)$, on the solid boundary and the free surface and the angle, θ, on the free surface, respectively.

3 The iterative procedure

The integral equations (18)-(22) are solved by employing the numerical iterative procedure developed by Wen and Ingham[7] as follows:

(a) Assume an initial profile for the free surface Γ_2. Distribute the grid points on the solid boundary Γ_1 and the free surface Γ_2.

(b) Assume an initial fluid speed distribution $u^n(s)$ ($= U_\infty$, say) on the solid boundary AB. Initially $n = 0$.

(c) The fluid speed, $u_f^n(s)$, on the free surface Γ_2 is calculated by using equation (25). Then $\phi^n(s)$, on Γ_1 and Γ_2 is calculated using equation (18).

(d) On substituting the values of β, $u_f^n(s)$ and $\phi^n(s)$ into the right hand sides of equations (21) and (22), new predictions for the fluid speed, $u^{n+1}(s)$, and the angle of the free surface, $\theta^{n+1}(s)$, are obtained.

(e) Using expressions (19) and (20), a new prediction for the free surface profile is determined.

(f) Steps (c) to (e) are repeated until the fluid speed, $u^n(s)$, and the velocity potential, $\phi^n(s)$, converge to within some specified limits.

4 Numerical results and discussion

The numerical calculations were performed for a step of variable height and inclination when the upstream Froude number is great than unity. Particular attention has been paid to the effects of varying h_s, β and Fr on the free surface profile. One of the main interests in this paper is also to reveal the mechanism for the occurrence of waves on the free surface.

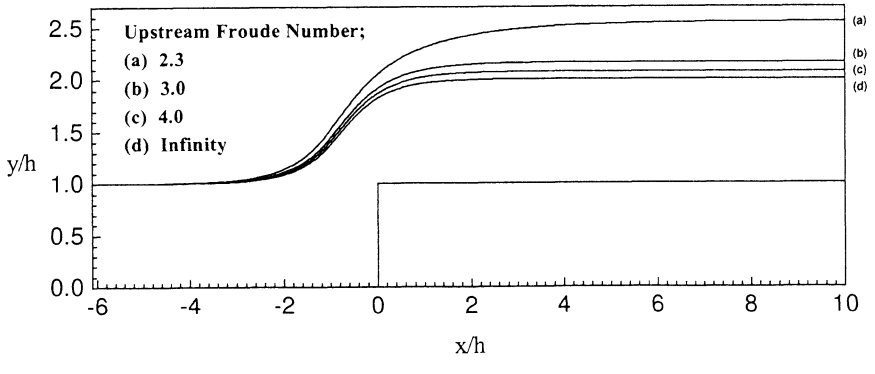

Figure 2: The free surface profiles for Froude numbers of ∞, 4.0, 3.0 and 2.3 when the step height is unity and the step angle is $\pi/2$.

Figure 2 shows a comparison of the free-surface profiles for different upstream Froude numbers of ∞, 4.0, 3.0 and 2.3 over a step when $h_s/h = 1.0$ and for a step angle of $\beta = \pi/2$ where it is served that there is a monotonic

increase in the height of the free-surface as the upstream Froude number reduces from infinity to 2.3.

Solutions for the fluid flow over a range of step angles, namely $\pi/8$, $\pi/4$, $\pi/2$, for an upstream Froude number Fr = 3.0 and $h_s/h = 1.0$ are given in Figure 3. In comparison with Figure 2, a feature that stands out in Figure 3 is the change in the shape of the free-surface as the step angle increases. The shape of the free-surface shows the greatest change is in the region just above its corresponding step and on increasing the angle of the step produces a steeper free surface near to the step.

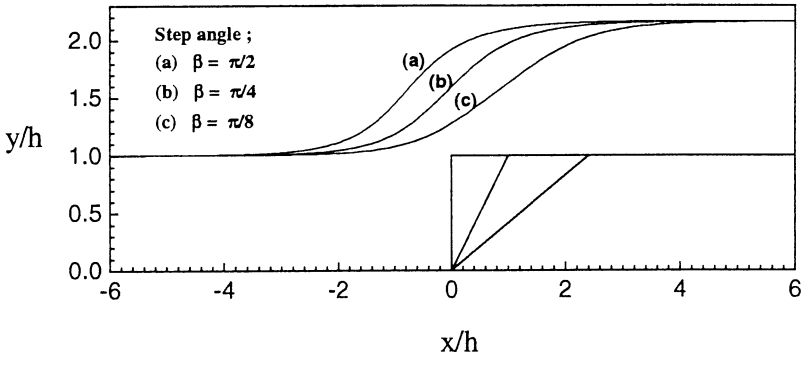

Figure 3: The free surface profiles for a Froude number of 3.0 when the step height is unity for step angles $\pi/8$, $\pi/4$, $\pi/2$.

Figure 4 shows a comparison of the free surface profiles for an upstream Froude number of 2.0 over step of height $h_s/h = 0.2$, 0.4 and 0.6 and 0.6188, and a step angle of $\beta = \pi/2$. As the step height increases the free surface height increases. When $h_s/h = 0.2$, the maximum free surface height obtained by King and Bloor[3] was found to be $y_f/h = 1.2744$ which compares favourably with the present prediction of $y_f/h = 1.2777$. Other values for the greatest free-surface elevation for step heights of 0.4, 0.6 and 0.6188 are also in good agreement with the values obtained by King and Bloor but these values can only be found by reading values from their figures. The maximum step height reached by King and Bloor was 0.6188, above which no solution could found. It led them to conclude that when the height is larger than this value then waves must occur on the free surface. Forbes[4] suggested that waves occur at some point at which the angle of the free surface is 30^0. However, the calculations of King and Bloor[3] did not support this suggestion and neither did our calculations. In our calculations the convergence of the iterative scheme becomes very difficult when the height of the step is slightly larger than 0.6188. A question of particular importance is what is the mechanism which leads to wavelike free surface flows and what is the critical step height at which waves first occurs. In

order to reveal this mechanism we define the local Froude number as

$$Fr_l(x) = u_f(x)/\sqrt{g[y_f(x) - y_b(x)]} \tag{26}$$

where $y_b(x)$ is the coordinate of the solid boundary, and therefore, $y_f(x) - y_b(x)$ is local depth of fluid.

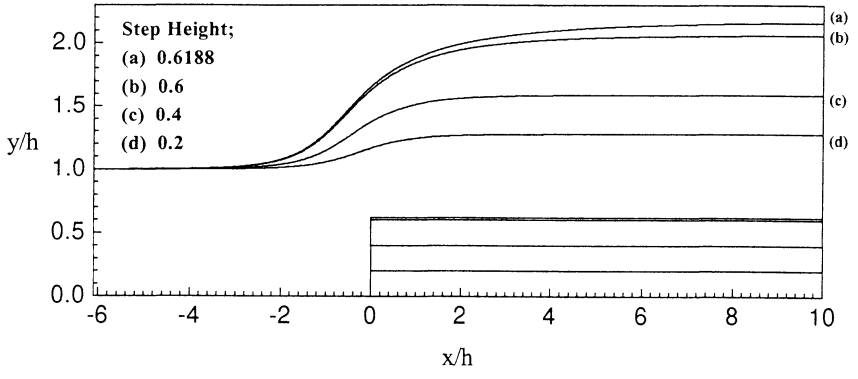

Figure 4: The free surface profiles for a Froude number of 2.0 when the step height is 0.2, 0.4, 0.6 and 0.6188 and the step angle is $\pi/2$.

Figure 5 shows the variation of the local Froude number $\mathrm{Fr}_l(x)$ as a function of the x co-ordinate for Fr = 2.0 at four different step heights, namely h_s/h = 0.6058, 0.6159, 0.6208 and 0.6245. The value of $\mathrm{Fr}_l(x)$ for all four curves far upstream of the step is 2.0, and as expected, each curve follows a similar path until the flow reaches the vicinity of the step. Infront of the step the local Froude number is always larger than unity. Beyond the step, the local Froude number rapidly decreases as the free-surface height increases. When the step height is less than 0.6058 the local Froude number monotonically decreases and it takes a minimum value far downstream of the step. However, when the step height reaches a 0.6058, then the local Froude number reaches a minimum somewhere downstream of the step and then begins to increase monotonically to its asymptotic value. When the step height is less than 0.6208 the local Froude number is always larger than unity and this indicates the the whole fluid flow is supercritical. When the step height is 0.6208 then the minimum value of the local Froude number is unity at x = 14.5. When the step height is slightly larger than 0.6208, say h_s/h = 0.6245, the local Froude number is less than unity in a large region, namely when $x \leq 5.75$ the flow is supercritical , when x = 5.75 the flow becomes subcritical and becomes again supercritical at x = 14.5. As is well known, waves occur when flow transfers from being supercritical to subcritical. Therefore, we conclude that for step heights less than 0.6208 then the minimum local Froude number is larger than unity and no waves may occur on the free surface. However, for step heights larger than 0.6208

the minimum value that the local Froude number takes is less than unity and waves must occur. Clearly, the critical step height is $h_s = 0.6208$, where the minimum of the local Froude number is unit. This value is very close to the critical height of 0.6188 predicted by King and Bloor, which indicates that transition of flow from superctical to subcritical is the reason why no solution could be found by King and Bloor when the minimum value of of local Froude number becomes less than one. Close agreement in the predicted maximum step height as obtained by both sets of results suggests that when the local Froude number reaches a value of unity, we can predict the critical step height and the maximum free-surface elevation over a step at different inclinations in the transitional region of subcritical and supercritical free-surface flow.

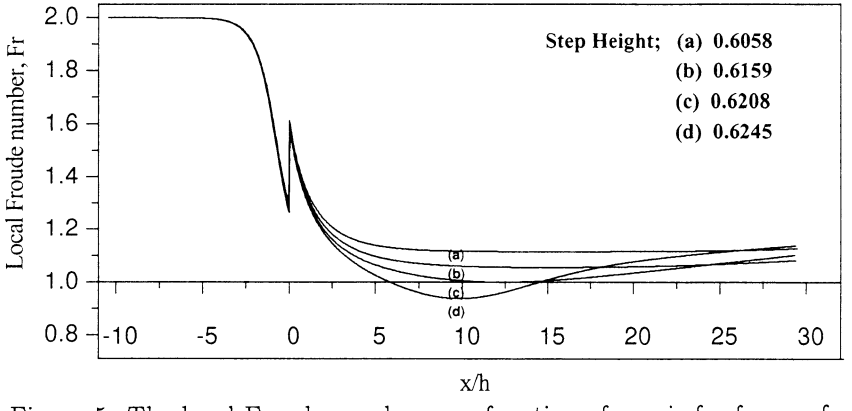

Figure 5: The local Froude number as a function of x-axis for free surface flows for an upstream Froude number 2.0 and step angle $\pi/2$ for h_s/h 0.6058, 0.6159, 0.5208 and 0.6245.

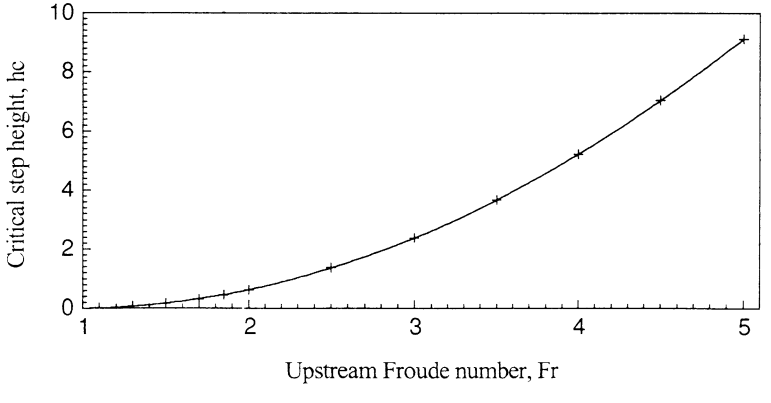

Figure 6: The local Froude number for free surface flow when the upstream Froude number is 2.0 and the step angle is $\pi/2$.

In a similar manner to that described in the previous paragraph, the critical step height h_c/h for various values of upstream Froude numbers have been calculated for free-surface flow over a step of inclination $\beta = \pi/2$. Figure 6 shows the critical step height as a function of the upstream Froude number and this indicates that the critical height is zero when Fr = 1.0 and it increases as the upstream Froude number increases.

5 Conclusion

A boundary integral technique has been developed for two-dimensional, free surface flows over a step in a two-dimensional channel and it has been applied to predict the free-surface profiles when the upstream flow is super-critical, namely, Fr $\geq$ 1.0. The mechanism for the occurrence of waves on the free surface is revealed by considering the local Froude number. This indicates that the criteria for waves to start to occur is that the local Froude number reaches a value of unity.

References

1. Varoglu, E. and Finn, W. D. L., Variable domain finite element analysis of free surface gravity flow, *Computers and Fluids*, 1978, **6**, 103-114.

2. Cheng, A. H-D., Liggett, J. A. and Liu, P. L-F., Boundary calculations of sluice and spillway flows, *J. Hydraulics Division*, ASCE, 1981, **107**, 1165-1178.

3. King, A. C. and Bloor, M. I. G., Free-surface flow over a step, *J. Fluid Mech.*, 1987, **182**, 193-208.

4. Forbes, L. K., Free-surface flow over a semi-circular obstruction, *J. Fluid Mech.*, 1982, **114**, 299-314.

5. Dias, F. and Vanden-Broeck, J. M., Flows over rectangular weirs, *J. Fluid Mech.*, 1989, **206**, 155-170.

6. Wen, X. and Wu, C., Boundary integral equation inverse method for free surface gravity flows, *Sciential Sinica*, Series A, 1987, **30**, 992-1008.

7. Wen, X. and Ingham, D. B., Flow induced by a submerged source or sink in a three-layer fluid, *Computers and Fluids*, 1992, **21**, 133-144.

8. Muskhelishvili, N. I., *Singular Integral Equations*, (Trans. and edited by Radok, J. R. M., Noordhoff, T.), Holland, 1953.